105 (2026) 106951

Contents lists available at ScienceDirect

Poultry Science

journal homepage: www.elsevier.com/locate/psj

Full-Length Article

Single-cell landscape of goose thymus uncovers developmental and regulatory dynamics of T cell differentiation

Cui Wang [a,†], Zuoyin Zhu [b,†], Yi Liu [a], Yongping Yang [c], Shufang Chen [d], Daqian He [a,*]

[a] Institute of Animal Science and Veterinary Medicine, Shanghai Academy of Agricultural Sciences, Shanghai 201106, China
[b] Department of Hematology, Tongji Hospital, Frontier Science Center for Stem Cell Research, School of Life Sciences and Technology, Tongji University, Shanghai 200092, China
[c] Wuhan Animal Disease Control Center, Wuhan 430012, China
[d] NingBo Academy of Agricultural Sciences, Ningbo 315040, China

ARTICLE INFO

Keywords:
Goose thymocyte development
Single-cell transcriptomics
T cell commitment
Cross-species comparison

ABSTRACT

The thymus is vital for T cell development, yet avian thymocyte maturation remains poorly characterized. Here, we present a single-cell transcriptomic atlas of thymic development in Zhedong White geese across embryonic, gosling, juvenile, and adult stages. Morphological and histological analysis revealed a multilobulated, paired thymus with rapid post-hatch expansion and age-dependent involution. Single-cell RNA sequencing identified all major thymic cell types, with T cells predominant and γδ T cells unusually abundant compared to mammals. High-resolution profiling defined key T cell subsets and reconstructed sequential differentiation, showing DN cells transition from pre-commitment states marked by BCL11A, SPI1, and HHEX to committed states (BCL11B, TCF7) and β-selection gene activation. Thymic epithelial cells functioned as central signaling hubs, mediating microenvironmental regulation. Comparative analysis with human and mouse thymus revealed a conserved developmental framework, yet pronounced species-specific differences at the DP stage and in γδ T cell enrichment. These findings contribute foundational insights for avian immunology and poultry breeding.

Introduction

The thymus is the central immune organ in vertebrates and serves as the primary site for T lymphocyte development, differentiation, and maturation (Medeiros et al., 2025). Within the thymus, hematopoietic progenitors undergo a highly ordered developmental program that integrates lineage commitment, antigen receptor gene rearrangement, and selection events, ultimately establishing a functional T-cell repertoire composed of $CD4^+$ and $CD8^+$ T cells as well as regulatory T cells (Ciofani and Zúñiga-Pflücker, 2007; P. M. Rodrigues et al., 2025). Through positive and negative selection, the thymus ensures that mature T cells acquire the capacity to recognize foreign antigens while maintaining tolerance to self-antigens (Klein et al., 2014). Mature T cells play critical roles in host defense against infection, tumor immunity, and immune homeostasis, and their proper development is essential for the establishment and long-term maintenance of an effective immune system (Eickhoff et al., 2015; Shim et al., 2022). Thymic development and T-cell differentiation are not governed solely by cell-intrinsic programs but instead depend on the fine regulation of the thymic microenvironment (Takahama, 2006). Multiple thymic stromal components act in concert with intrinsic differentiation programs to provide essential support for thymocyte migration, selection, and maturation (Pedro M. Rodrigues et al., 2025). Disruption of this regulatory system can lead to aberrant T-cell development and subsequently contribute to the onset of immune-related diseases, including immunodeficiency, autoimmunity, and immune aging (Palmer, 2013). Therefore, elucidating the molecular regulatory mechanisms underlying thymic development from a systems-level perspective is of fundamental importance for understanding adaptive immune homeostasis and the pathogenesis of immune-associated disorders (Takaba and Takayanagi, 2017).

The application of single-cell RNA sequencing has enabled the dissection of thymic cellular heterogeneity, developmental trajectories, and regulatory networks at single-cell resolution, thereby refining and extending the classical "DN–DP–SP" framework of T-cell differentiation (Kernfeld et al., 2018; Li et al., 2021). Related studies have shown that T-cell fate determination and development are jointly regulated by the

* Corresponding author at: Shanghai Academy of Agricultural Sciences, Beidi Road No. 2901, Shanghai, PR China.
E-mail address: shwaterfowl@163.com (D. He).
† These authors contributed equally.

https://doi.org/10.1016/j.psj.2026.106951
Received 29 January 2026; Accepted 16 April 2026
Available online 17 April 2026

NOTCH signaling pathway, key transcription factors such as GATA3, TCF7, and BCL11B, as well as tightly controlled T-cell receptor (TCR) signaling (Rothenberg et al., 2008; Yui and Rothenberg, 2014). Meanwhile, substantial interspecies differences persist in developmental timing, lineage bias (e.g., αβ versus γδ T cells), and microenvironmental regulation, and these factors collectively shape species-specific immune strategies (Boehme et al., 2022; Flajnik and Kasahara, 2010). In contrast, systematic studies of thymic development in birds remain limited. The avian immune system exhibits distinct phylogenetic features, including the bursa of Fabricius as the central organ for B-cell development and the absence of classical lymph nodes, suggesting that immune developmental regulation in birds may differ from that in mammals (Ratcliffe, 2006). Existing studies have largely relied on anatomical and histological analyses with limited marker-based resolution, leaving the dynamic cellular composition and regulatory programs of the avian thymus poorly characterized (Ribatti et al., 2019). Consequently, mammalian developmental paradigms cannot be directly extrapolated to birds, underscoring the need for systematic investigation of avian thymic development (Chen et al., 1990).

The domestic goose (Anser cygnoides) is an economically important waterfowl species, and global goose meat production is projected to reach 4.751 million tons by 2027, highlighting its increasing importance for animal protein supply and rural economic development (Dumlu, 2024). The Zhedong White (ZW) goose, a representative indigenous breed, is valued for its favorable production performance and environmental adaptability, and plays an important role in the conservation and utilization of local poultry genetic resources (Ren et al., 2016). Beyond their economic importance, birds exhibit immune features that differ from those of mammals in certain viral infections, with accumulating evidence indicating distinct antiviral responses (Campbell and Magor, 2020; Webster et al., 1992). However, studies of goose thymic development remain limited and lack systematic cellular and molecular characterization. In this context, a systematic investigation of goose thymic development from agricultural and comparative immunology perspectives can deepen our understanding of avian immune diversity and provide insights into stage-dependent vaccine responses, with potential implications for optimizing immunization strategies.

To address the limited understanding of avian thymic T cell development, this study employed the ZW goose as a representative waterfowl model and analyzed thymic development across four key stages: embryos at 25 days old (E25), goslings at 14 days post-hatch (D14), juvenile geese at 70 days post-hatch (D70), and laying geese at 200 days post-hatch (D200), corresponding to thymus formation, early immune establishment, immune homeostasis, and post–sexual maturity maintenance, respectively. By integrating histological and morphological analyses with single-cell transcriptomics, trajectory inference, and gene regulatory network analysis, this study aimed to characterize dynamic thymic development, construct a single-cell atlas, delineate T cell differentiation trajectories and regulatory programs, and identify conserved and species-specific features through cross-species comparison. Collectively, this work provides a comprehensive framework for understanding avian thymic T cell development and offers a valuable resource for comparative immunology and disease-resistant poultry breeding.

Materials and methods

Animal ethics

All animal experiments and procedures conducted in this study were approved by Animal Care and Use Committee of Shanghai Academy of Agricultural Sciences (License No. SAASXM0523005) and were performed in accordance with its ethical guidelines and regulations.

Experimental design and thymus sample collection

This study used female ZW geese at four developmental stages: E25, D14, D70 and D200. All animals were provided by the Wenjie Goose Breeding Department of Xiangshan Co., Ltd. (Ningbo, China). Fertilized eggs were incubated using a commercial incubator (Zhonglian, China). Goslings were raised in a brooding house, while geese at D70 and D200 were reared under standard commercial farming conditions. The thymus in geese is bilaterally situated in the neck region and typically consists of 4–6 lobes on each side. At each time point, thymus samples were randomly collected from three individuals and fixed in 0.4% paraformaldehyde (Servicebio, Wuhan, China) for histological analysis. In parallel, thymus samples from an additional three geese were preserved in MACS Tissue Storage Solution (Miltenyi Biotec, Germany) and used for thymic cell isolation and single-cell RNA sequencing. Sex was verified through PCR amplification of the CHD-1 gene (Lai et al., 2022) (Fig. S1 and Table S1).

Thymus index measurement and histological analysis

Prior to euthanasia, geese were fasted for 24 h and their body weight was recorded. Thymus tissues were aseptically excised and weighed. The thymus index was calculated as the ratio of thymus weight (g) to body weight (g). For histological analysis, thymus samples were fixed in 4% paraformaldehyde for 24 h, embedded in paraffin, and sectioned at 5 μm thickness. Tissue sections were deparaffinized in xylene, rehydrated through a graded ethanol series, and stained with hematoxylin and eosin (H&E) as previously described (Li et al., 2020). Thymic microstructure was examined and imaged under a light microscope (Olympus, Japan).

Thymocyte isolation and scRNA-seq library construction

Thymus tissues were minced on ice, washed with 1× PBS, and dissociated into single-cell suspensions using a dissociation solution at 37°C for 20 min with gentle shaking. Digestion was stopped by adding PBS supplemented with 10% fetal bovine serum (FBS). The resulting suspensions were filtered through a 40- μm cell strainer, centrifuged at 300 × g for 5 min at 4°C, and resuspended in PBS containing 0.04% bovine serum albumin (BSA). Residual red blood cells were removed using 1×red blood cell lysis buffer (Invitrogen, USA). Cell viability was determined by trypan blue exclusion, and only samples with viability exceeding 85% were used for downstream processing. Single-cell suspensions were adjusted to a concentration of 400–1,200 cells/μL and processed on the 10× Genomics Chromium platform using the Chromium Single Cell 3′Library Kit (v3) following the manufacturer's instructions. Libraries were sequenced on an Illumina NovaSeq 6000 system in paired-end 150-bp mode by Shanghai Personal Biotechnology Co., Ltd. (Shanghai, China) (Zheng et al., 2017).

Single-cell RNA-seq data processing and analysis

Raw FASTQ sequencing data from goose thymic samples were processed using Cell Ranger (v7.1.0, 10× Genomics) with default parameters and aligned to the goose reference genome (GCF_002166845.1, Goose v1.0) (Zheng et al., 2017). The resulting gene-cell expression matrices were imported into Seurat (v5.3.1) for downstream analysis (Stuart et al., 2019). Quality control was performed based on the number of detected genes, total UMI counts, and the proportion of mitochondrial gene expression. Cells with fewer than 300 or more than 6,500 detected genes, fewer than 1,000 or more than 50,000 UMIs, or mitochondrial gene content exceeding 20% were removed. Mitochondrial genes were annotated based on the published complete mitochondrial genome of Bean goose (Liu et al., 2013). Potential doublets were identified and removed with scDblFinder (1.22.0) (Germain et al., 2021). After quality control, the data were normalized and scaled while regressing out mitochondrial effects. Highly variable genes were

identified, followed by Principal Component Analysis (PCA) and Harmony-based batch integration. Cell populations were subsequently identified through graph-based clustering in Seurat (Korsunsky et al., 2019). Low-dimensional visualization was performed using Uniform Manifold Approximation and Projection (UMAP) and t-distributed Stochastic Neighbor Embedding (t-SNE). Differential gene expression between clusters was evaluated via the Wilcoxon rank-sum test, with an adjusted $P < 0.05$ considered statistically significant.

Pseudotime analysis of thymic T-cell development

Pseudotime analyses were performed using Monocle3 (v1.4.26) and Monocle2 (v2.36.0) to reconstruct the developmental dynamics of thymic T cells (Cao et al., 2019; Qiu et al., 2017). Cells annotated as ISP, DP, late DP, CD4SP, CD8SP, and Treg were subsetted from the Seurat object, reprocessed (including LogNormalize, variable feature selection, scaling, and PCA), and used for UMAP reconstruction (Stuart et al., 2019). A Monocle3 cell_data_set was generated from raw UMI counts and cell metadata, utilizing Seurat-derived UMAP embeddings for trajectory inference. Cell clustering was performed with the cluster_cells function, and developmental trajectories were learned via learn_graph. Pseudotime values were assigned using order_cells and visualized with plot_cells (Cao et al., 2019).

For early developmental stages, DN thymocytes were analyzed using Monocle2. A CellDataSet was constructed from raw UMI counts based on a negative binomial model (Trapnell et al., 2014). Ordering genes were defined by integrating DN markers, variable features from Seurat, and highly dispersed genes. Trajectories were reconstructed using DDRTree algorithm, and cells were ordered with orderCells function (Qiu et al., 2017). Genes associated with pseudotime progression were identified through differentialGeneTest and visualized in pseudotime heatmaps.

SCENIC analysis of DN-stage T-cell transcriptional regulation

SCENIC analysis (v1.3.1) was performed to characterize transcriptional regulatory programs during the DN1–DN3b stages of double-negative (DN) T-cell development. DN cells were extracted from the Seurat object, and raw UMI count matrices were used as input. Because no established poultry-specific SCENIC motif database is currently available, an ortholog-based strategy was applied to improve compatibility with existing regulatory resources. Specifically, goose genes were mapped to strict one-to-one human orthologs using biomaRt (v2.64.0) based on Ensembl annotations, and goose gene symbols were replaced with the corresponding human gene symbols for downstream analysis. This mapping yielded 11,996 orthologous genes (Table S2) (Durinck et al., 2009).

The analysis followed the standard SCENIC workflow: lowly expressed genes were filtered using geneFiltering function, gene co-expression networks were inferred with GENIE3, and candidate regulons were defined by integrating co-expression modules with cis-regulatory motif enrichment using RcisTarget (hg19 motif database, scanning regions 500 bp upstream and ±10 kb around transcription start sites). Regulon activity was quantified at the single-cell level using AUCell and subsequently incorporated into the Seurat object. Stage-specific and cell-specific regulon dynamics of regulons were visualized using boxplots, UMAP projections, and heatmaps (Aibar et al., 2017). Given the use of human regulatory databases, this analysis was intended primarily to identify conserved regulatory trends and candidate regulators rather than to comprehensively resolve poultry-specific regulatory interactions.

Cell-cell communication analysis

Cell-cell communication analysis was performed using the CellChat R package (v1.6.1) (Jin et al., 2021). A Seurat object containing annotated thymic epithelial cells and T-cell subsets served as input. To enhance the accuracy of ligand–receptor pairing, goose genes were mapped to their human orthologs based on one-to-one orthologous relationships identified using biomaRt, yielding 11,996 conserved orthologous gene pairs (Table S2). CellChat objects were constructed from the normalized expression matrix and cell-type annotations, and the human CellChat ligand–receptor database was applied for downstream analysis.

Communication inference followed the standard CellChat workflow, which included identification of overexpressed genes and ligand–receptor interactions, calculation of communication probabilities, filtering of low-abundance interactions, and pathway-level aggregation. Communication networks were visualized using circle plots, bubble plots, signaling role heatmaps, and pattern-based decomposition analyses.

Cross-species integration and comparative analysis of thymic single-cell transcriptomes

Human thymic single-cell RNA-seq data were obtained from GSA-Human (HRA007980). Samples from embryonic week 17 (E17), postnatal 4 months (4 M), 39 years (39Y), and 60 years (60Y) were selected to cover the major stages of human thymic T cell development(Li et al., 2024). Mouse thymic single-cell RNA-seq data were retrieved from ArrayExpress (E-MTAB-8581), covering embryonic day 12-18 (E18), postnatal day 1, 4 weeks (4 W), 8 weeks (8 W), and 24 weeks (24 W), thereby spanning the full course of mouse thymic development (Kernfeld et al., 2018; Park et al., 2020).

To enable cross-species comparability among goose, human, and mouse thymic cells, gene mapping was performed using biomaRt (v2.64.0) based on strict one-to-one orthologous relationships defined in the Ensembl database. Human and mouse gene identifiers were converted to their corresponding goose gene symbols, and only genes shared across all three species with one-to-one orthology were retained to construct a common feature space, yielding a total of 11,882 conserved orthologous genes (Table S3).

After re-identification of 3,000 highly variable genes and PCA, cross-species batch effects were corrected using Harmony, followed by graph-based clustering and UMAP/t-SNE visualization. Within each cell type, Goose vs Human and Goose vs Mouse differential expression analyses were performed using Seurat (Wilcoxon test; $|\log2FC| > 0.25$, FDR < 0.05), and significant genes were summarized using pseudo-bulk Z-score–scaled heatmaps.

Results

Morphology and histological development of the thymus in ZW geese

The thymus in ZW goose consists of 4-6 pairs of irregular lobes arranged in two bilateral chains along the neck (Fig. 1A, Table S4). Its development follows a distinct age-dependent trajectory. At embryonic day 25 (E25), the thymus is morphologically identifiable. It undergoes rapid expansion after hatching, reaching peaking absolute weight at D70, followed by pronounced atrophy byD200 (Fig. 1B). Histological analysis (Fig. 1C) revealed corresponding architectural maturation: from initial cortico-medullary separation at E25, to clear demarcation and medullary expansion by D14, advanced lobular organization at D70, and finally cortical thinning with signs of involution at D200. This pattern mirrors the conserved vertebrate sequence of thymic growth, maturation, and physiological regression.

Single-cell transcriptomic profiling reveals dynamic cellular composition during goose thymus development

Single-cell RNA sequencing (scRNA-seq) was performed on goose thymus at E25, D14, D70, and D200 to characterize thymic cellular dynamics (Fig. 2A). Across all stages, high-quality data were obtained

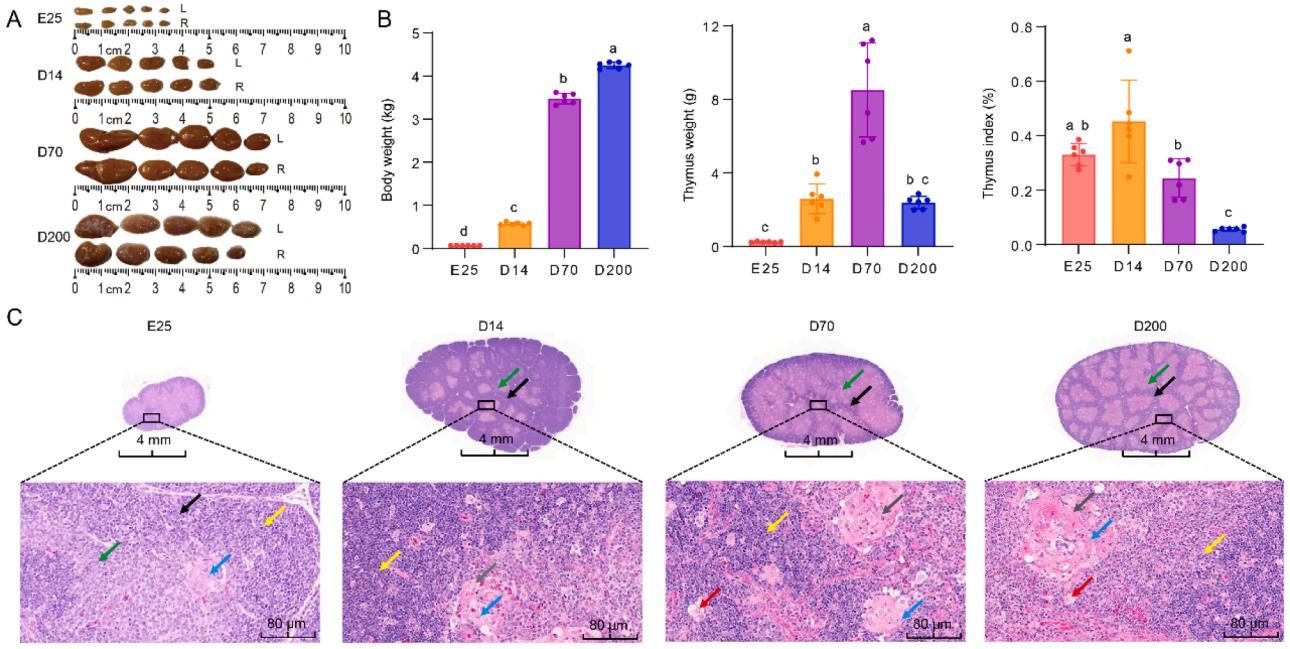

Fig. 1. Age-associated morphological and histological changes in the thymus of ZW goose. (A) Representative photographs of unilateral thymic lobes at four developmental stages: embryos at 25 days old (E25), goslings at 14 days post-hatch (D14), juvenile geese at 70 days post-hatch (D70), and laying geese at 200 days post-hatch (D200). One bird per stage is shown. (B) Body weight, absolute thymus weight, and thymus index (thymus weight/body weight × 100%). Data are presented as mean ± SD ($n = 6$). Different lowercase letters indicate significant differences among groups ($P < 0.05$), as determined by one-way ANOVA followed by Tukey's multiple comparisons test. (C) Representative hematoxylin and eosin (H&E)-stained thymic sections at low (10×, upper panels) and high (400×, lower panels) magnification. Black rectangles indicate the regions enlarged in the lower panels. Key structures are indicated: thymic medulla (green arrow); thymic cortex (black arrow); thymocyte (yellow arrow); thymic epithelial cell (light-blue arrow); thymic corpuscle (gray arrow); macrophage (red arrow). Scale bars are provided.

(average ~10,000 cells/stage; >91% reads confidently mapped; Table S5, Figure S2). After stringent filtering, 37,950 cells expressing 18,352 genes were analyzed (Fig. 2B).

Unsupervised clustering identified 11 cell clusters, classified into five major populations by canonical markers: T cells (clusters 0-5), B cells (6-7), macrophages (8), dendritic cells (9), and thymic epithelial cells (TEC; 10) (Fig. 2B and C). UMAP visualization confirmed discrete cell type-specific marker expression (Fig. 2D).

T cells constituted the majority at all stages (97.8% at E25, declining to 87.1% at D70, then rising to 92.2% at D200). B cell frequency increased post-hatch, peaking at D70 (10.7%) before decreasing, while myeloid and TEC populations remained stable but minor (Fig. 2E, Table S6). Distinct transcriptomes characterized each population: T cells (*CD8B, RAG1, DNTT*), B cells (*PAX5, EBF1, BCL11A*), myeloid cells (*C1QB, CSF3R, MAFB, ZNF366, FABP5*), and TECs *(LAMA4, SEMA3A, SOD3, FERMT2*) (Fig. 2F).

Collectively, these data demonstrate that the goose thymus is dominated by T cells, with dynamic shifts in B cell abundance post-hatch and relatively stable proportions of other non-T cell lineages, underscoring coordinated thymic maturation at single-cell resolution.

Single-cell transcriptomic atlas reveals T cell heterogeneity in the goose thymus

To resolve the diversity of thymic T cell populations in geese, we performed re-clustering of T cells, identifying transcriptionally distinct subsets (Fig. 3A and B, Figure S3): double-negative (DN), γδ T cells, immature single-positive (ISP), double-positive (DP), late DP, CD4 single-positive (CD4SP), CD8 single-positive (CD8SP), regulatory T cells (Treg), and cycling T cells.

Each subset displayed characteristic gene signatures. DN cells expressed early thymocyte markers (*KIT, RUNX1, CD44*) and V(D)J recombination genes (*DNTT, RAG1/2*). γδ T cells were marked by *SOX13, BLK*, and *RASGRP1*. ISP and DP cells expressed TCR maturation genes (*DNTT, RAG1/2, CD3D/E*). CD4SP and CD8SP subsets showed lineage-specific expression patterns: *CD4, TCF7*, and *GATA3* in CD4SP; *CD8A/B* and *RUNX3* in CD8SP. Treg cells were defined by *IL2RA, CTLA4, TNFRSF18*, and *TNFRSF4*, while cycling T cells highly expressed proliferation genes (*MKI67, TOP2A, PCNA, MCM6*).

Stage-specific frequency analysis (Fig. 3C, Table S7) revealed: DN cells were most prevalent at E25 and D14 but declined thereafter; γδ T cells represented a comparatively large and stable fraction (12.4-17.5%) across all stages—significantly higher than in mammals (~1-5%); DP cells dominated throughout development (30-50% of T cells); CD4SP and CD8SP frequencies increased with age, and Treg cells peaked at D70.

Trajectory analysis indicated a continuum from ISP to DP, branching into CD4SP and CD8SP lineages at the late DP stage (Fig. 3D). CD4SP cells preferentially expressed *CD4, GATA3, TCF7, KLF2, CCR7, S1PR1*, while CD8SP cells were enriched for *CD8A, CD8B*, and *RUNX3* (Fig. 3E).

Together, these data establish a single-cell atlas of goose thymic T cells, illuminating distinct developmental pathways and the notable expansion of avian γδ T cells relative to mammals.

Developmental trajectories and regulatory mechanisms of T cell lineage commitment and β-selection

To delineate the molecular events underlying early T cell commitment and β-selection, re-clustering of DN thymocytes identified five transcriptionally distinct stages: DN1, DN2a, DN2b, DN3a, and DN3b (Fig. 4A and B). Pseudotime analysis revealed a continuous developmental transition, with DN1 and DN2a representing early progenitors, progressing through DN2b to DN3a and terminal DN3b states (Fig. 4C and D; Figure S4A). Early-stage cells (E25, D14) predominated within early DN subsets (Fig. 4D, Figure S4B).

Three major pseudotime states were defined by the sequential regulatory of gene activation (Fig. 4D and E): State 1 was marked by expression of progenitor genes (*KIT, CD44*), State 2 by upregulation of

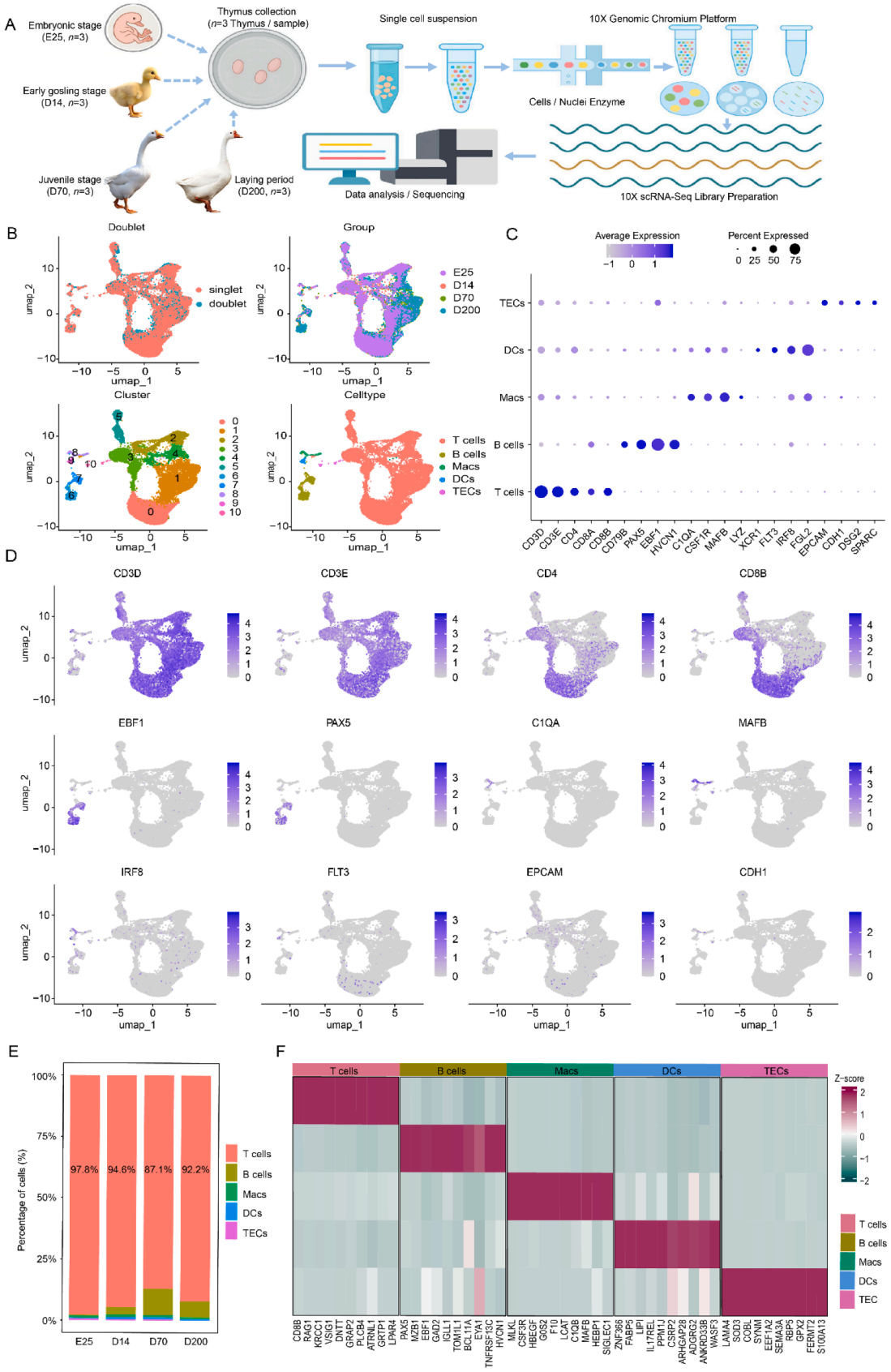

Fig. 2. A single-cell transcriptomic atlas of the goose thymus. (A) Overview of sample preparation, library construction, and scRNA-seq data analysis. (B) Uniform Manifold Approximation and Projection (UMAP) visualization of doublet detection, developmental stages, clustering, and celltype annotation. (C) Dot plot showing canonical marker gene expression across major thymic cell populations. (D) UMAP feature plots showing the spatial expression of representative marker genes. (E) Relative proportions of major thymic cell populations across developmental stages. (F) Heatmap showing the top 10 marker genes across major thymic cell populations.

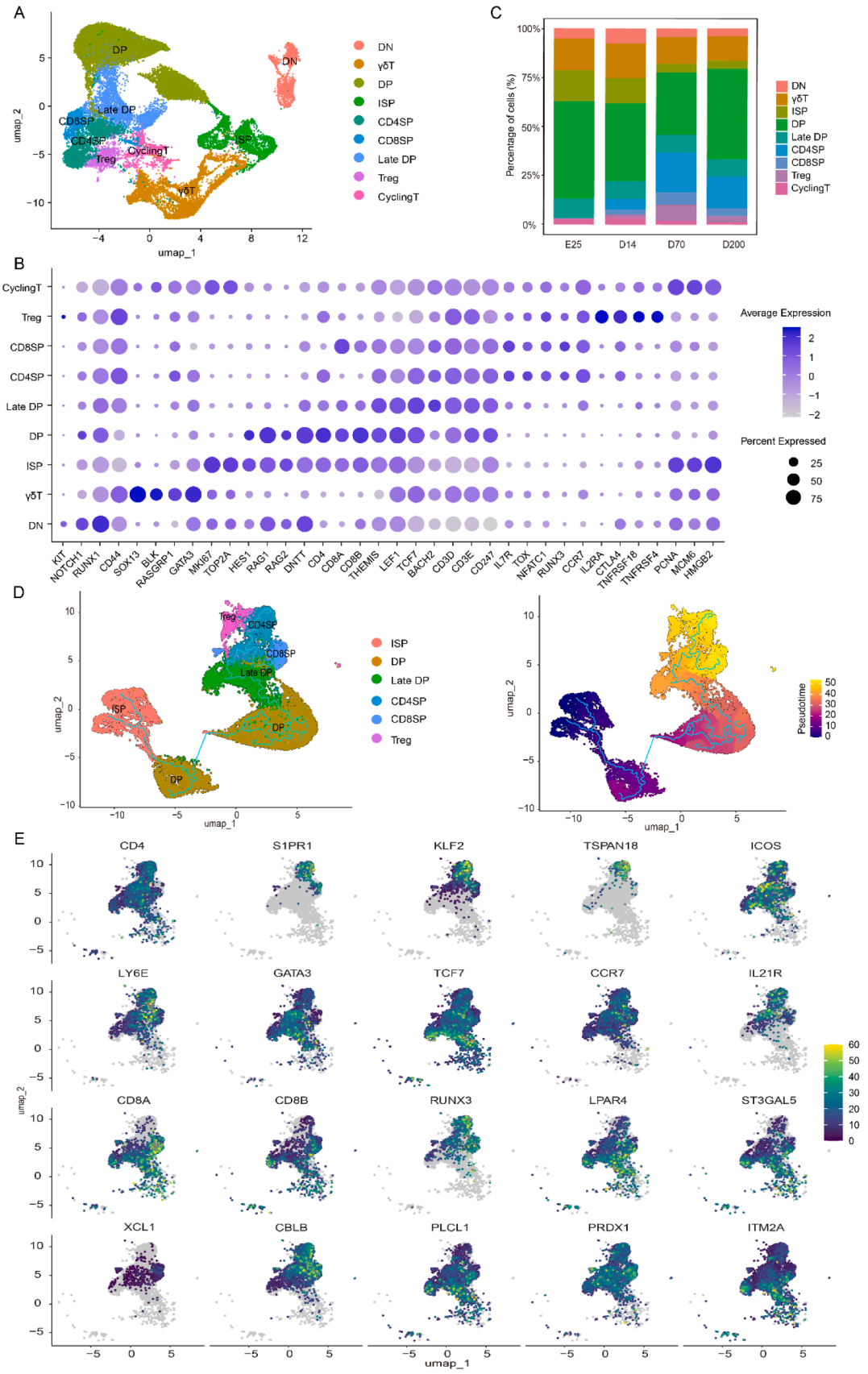

Fig. 3. Single-cell transcriptomic landscape and developmental trajectories of T cell populations in the goose thymus. (A) UMAP visualization of T cell type annotation in the goose thymus. (B) Dot plot showing marker gene expression across T cell subsets. (C) Stage-specific composition of T cell subsets across thymic development. (D) Trajectory inference of T cell differentiation during thymic development. (E) Expression of lineage-specific genes at the double-positive (DP) bifurcation toward CD4 single-positive (CD4SP) and CD8 single-positive (CD8SP) fates.

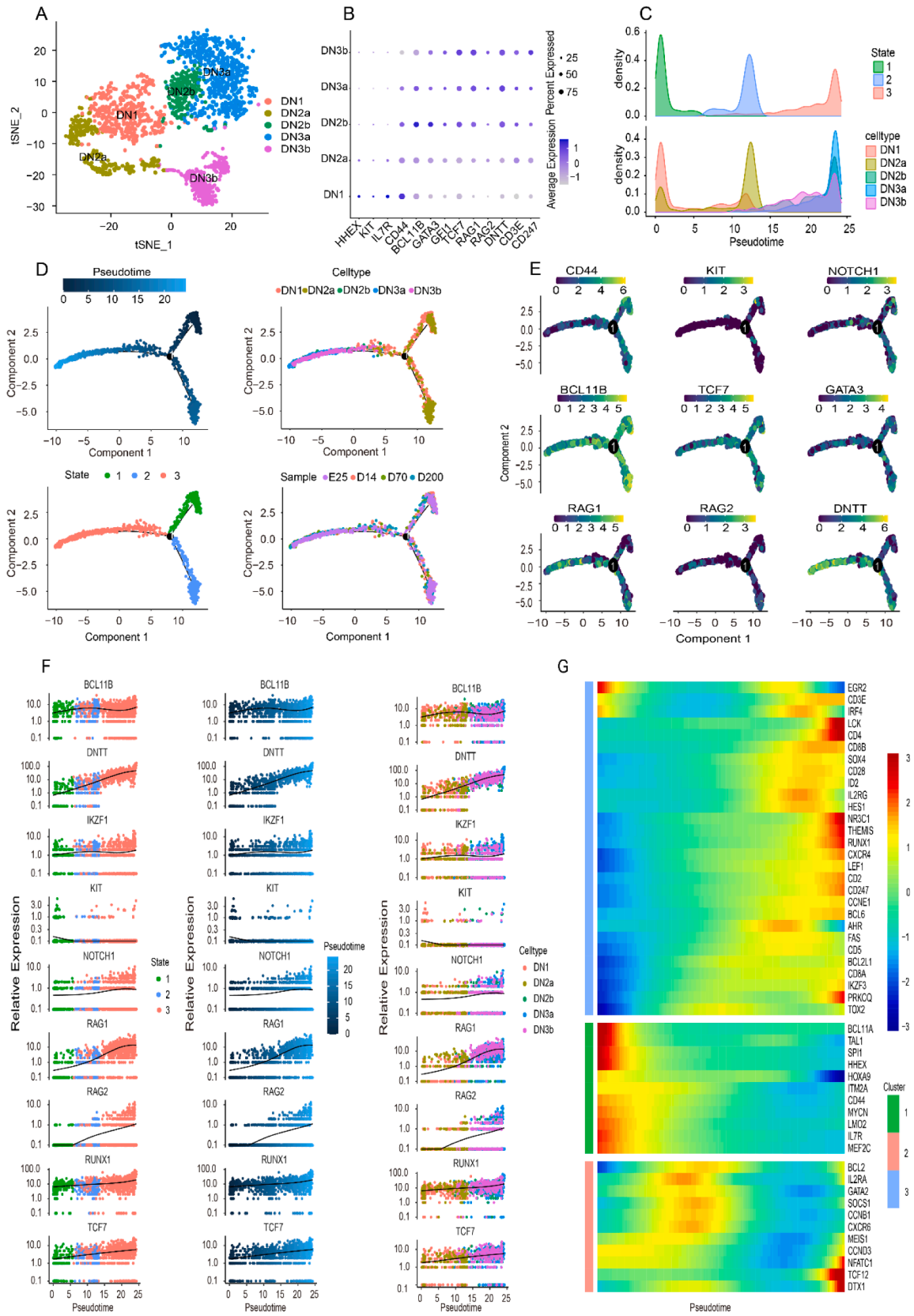

Fig. 4. Fine delineation and developmental trajectory analysis of DN cell subsets. (A) The t-distributed Stochastic Neighbor Embedding (t-SNE) visualization of double-negative (DN) cell subset heterogeneity in the goose thymus. (B) Dot plot showing expression of representative marker genes across DN cell subsets. (C) Pseudotime density distributions of DN cell subsets and developmental states. (D) Reconstruction of DN cell developmental trajectories using Monocle 2, illustrating pseudotime progression, cell-type distribution, trajectory states, and developmental-stage contributions. (E) Expression dynamics of key genes along the DN developmental trajectory. (F) Pseudotime-dependent expression dynamics of key regulatory and recombination-related genes during DN cell development. (G) Pseudotime resolved heatmap of dynamically expressed genes during DN cell development.

BCL11B (indicating T cell lineage commitment), and State 3 by induction of genes critical for TCR β-chain recombination (*RAG1, RAG2*, and *DNTT*)—hallmarking β-selection (Yui and Rothenberg, 2014; Rothenberg, 2019).

Temporal differential gene expression analysis identified three core modules (Fig. 4G): an early module of progenitor-associated transcription factors (e.g., *BCL11A, TAL1, SPI1, HHEX, HOXA9, LMO2*); an intermediate module linked to T cell identity and proliferation (*LEF1, TCF7, RUNX1, BCL2, CCNB*1, *IL2RA, SOCS1, DTX1, TOX2*); and a late module involved in TCR signaling and β-selection (*CD3E, CD3D, CD4, CD8B, IKZF3, PRKCQ, NFATC1*) (Fig. 4F and 4G).

In summary, these data reconstruct a detailed developmental trajectory and reveal stage-specific gene regulatory networks that orchestrate T cell lineage commitment and β-selection in the goose thymus.

SCENIC analysis reveals dynamic regulatory programs during DN thymocyte development

SCENIC analysis of goose DN thymocyte subsets delineated dynamic changes in transcription factor regulon activity during early T cell differentiation (Fig. 5A). At the DN1 stage, *CBFB* and *E2F7* regulons dominated, reflecting a highly proliferative and undifferentiated state (Kent and Leone, 2019). As cells progressed to DN2b, activation of lineage commitment regulons (*GATA3, TCF3, FOXP1*) marked the onset of T cell specification, with sustained activity into later DN stages.

Notably, *SOX13* regulon activity surged at the DN2b-DN3a transition, implicating *SOX13* in early γδ T cell lineage bias—a finding consistent with the substantial γδ T cell pool observed in the goose thymus (Melichar et al., 2007). Transitioning from DN3a to DN3b, *LEF1* and *TCF7* regulon activities increased markedly, indicating their roles in consolidating T cell commitment and initiating β-selection. Additionally, *SOX4* and *TCF12* regulons were persistently active throughout

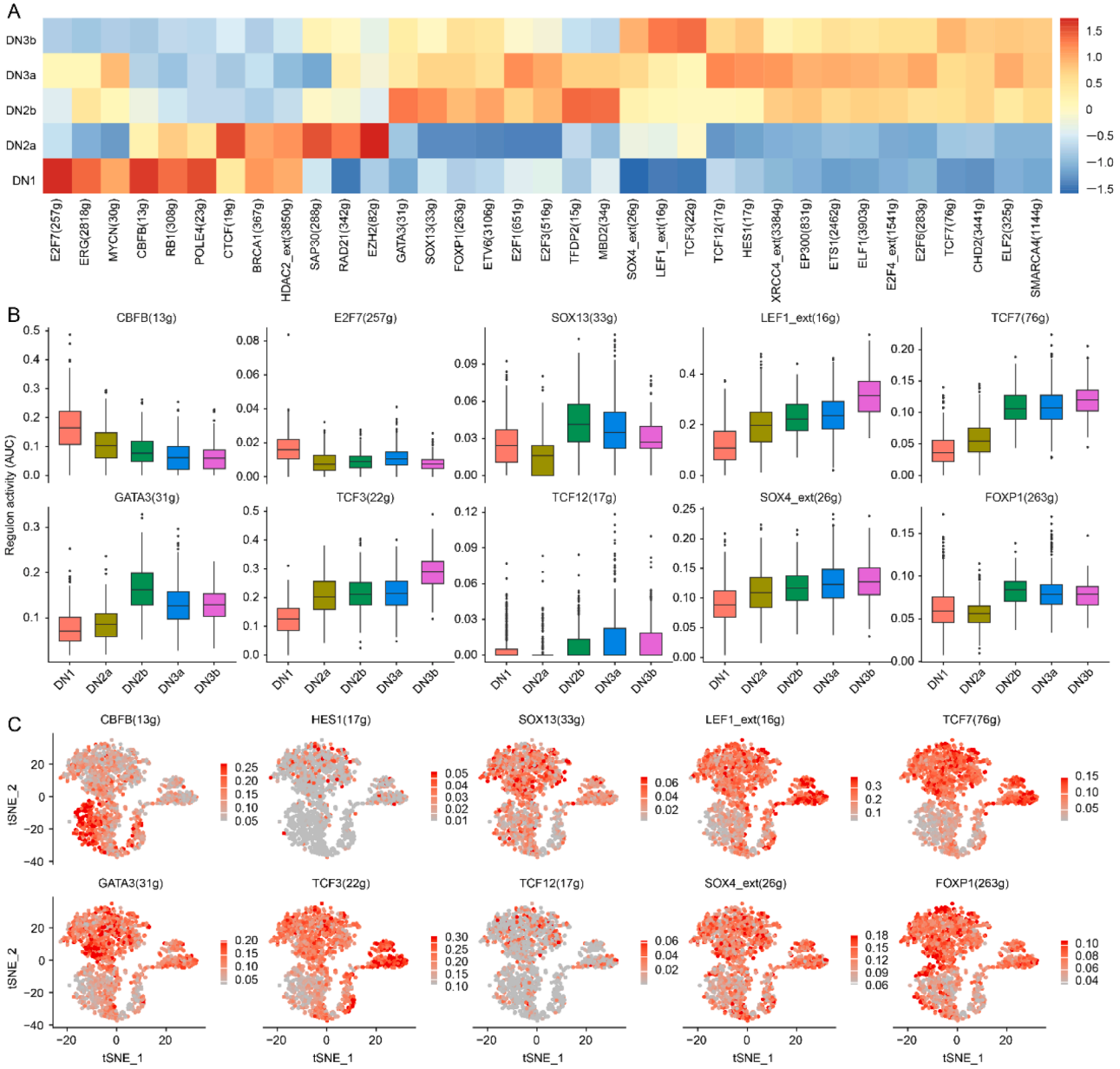

Fig. 5. SCENIC analysis reveals dynamic regulatory programs during the DN stage. (A) Dynamic activity of transcription factor regulons across DN cell subsets revealed by SCENIC analysis. (B) Differential regulon activity of key transcription factors across DN cell subsets. (C) The t-SNE visualization of key regulon activities across DN cell subsets.

DN3, suggesting involvement in late-stage differentiation (Fig. 5B). t-SNE mapping of regulon activities demonstrated a spatially continuous and gradual regulatory progression at single-cell resolution, emphasizing that DN differentiation is governed by coordinated, stepwise regulatory shifts rather than discrete transitions (Fig. 5C).

Collectively, these findings provide a comprehensive view of the regulatory network dynamics orchestrating DN thymocyte development and reveal key candidate regulators underlying avian T cell lineage commitment.

Cell-cell communication networks between TECs and T cell populations

Comprehensive analysis of cell-cell interactions in the goose thymus revealed that thymic epithelial cells (TECs) serve as a central signaling hub, engaging extensively with all major T cell subsets—including DN, ISP, DP, CD4SP, CD8SP, γδ T, and Treg cells (Fig. 6A). DP cells also exhibited high connectivity with CD4SP, CD8SP, and Treg populations, supporting a model in which TECs orchestrate continuous signaling during T cell maturation, with DP cells acting as intermediary nodes for thymic selection.

Signaling between TECs and T cells was primarily mediated by adhesion and microenvironmental ligand–receptor pairs (NAMPT-INSR, LAMC1/4-CD44, ALCAM-CD6). Robust CD99-CD99 homotypic interactions between TECs and γδ T cells highlighted specialized adhesion-mediated communication unique to this context (Fig. 6B).

Quantitative assessment showed that TECs were the principal source of outgoing signals, largely producing extracellular matrix and adhesion-related pathways (LAMININ, ALCAM, CDH), which were predominantly received by DN, γδ T, and SP T cells (Fig. 6C). T cell subsets displayed stage-specific signaling roles: IL16 was sent mainly by mature T cells to DP cells, while ICOS signals originated from DN cells to differentiated T cell subsets.

Communication clustering identified two main network modes (Fig. 6D): Pattern 1, dominated by DP, CD4SP, CD8SP, and Treg cells (IL16, NEGR, CD99, CD6, and ITGB2 signals), and Pattern 2, centered on TECs, DN, γδ T, and ISP cells (LAMININ, ICOS, SEMA4, ALCAM, VISFATIN, CDH). Correspondingly, signal reception patterns showed ISP, DP, CD4SP, CD8SP, and Treg cells were most responsive to IL16, LAMININ, and ICOS, whereas TECs, DN, and γδ T cells primarily responded to SEMA4, CD6, and CDH.

Overall, these results demonstrate a hierarchical communication network in which TECs and early T cell populations direct microenvironmental organization and signal production. In contrast, DP and differentiated T cell populations function as hubs for signal integration,

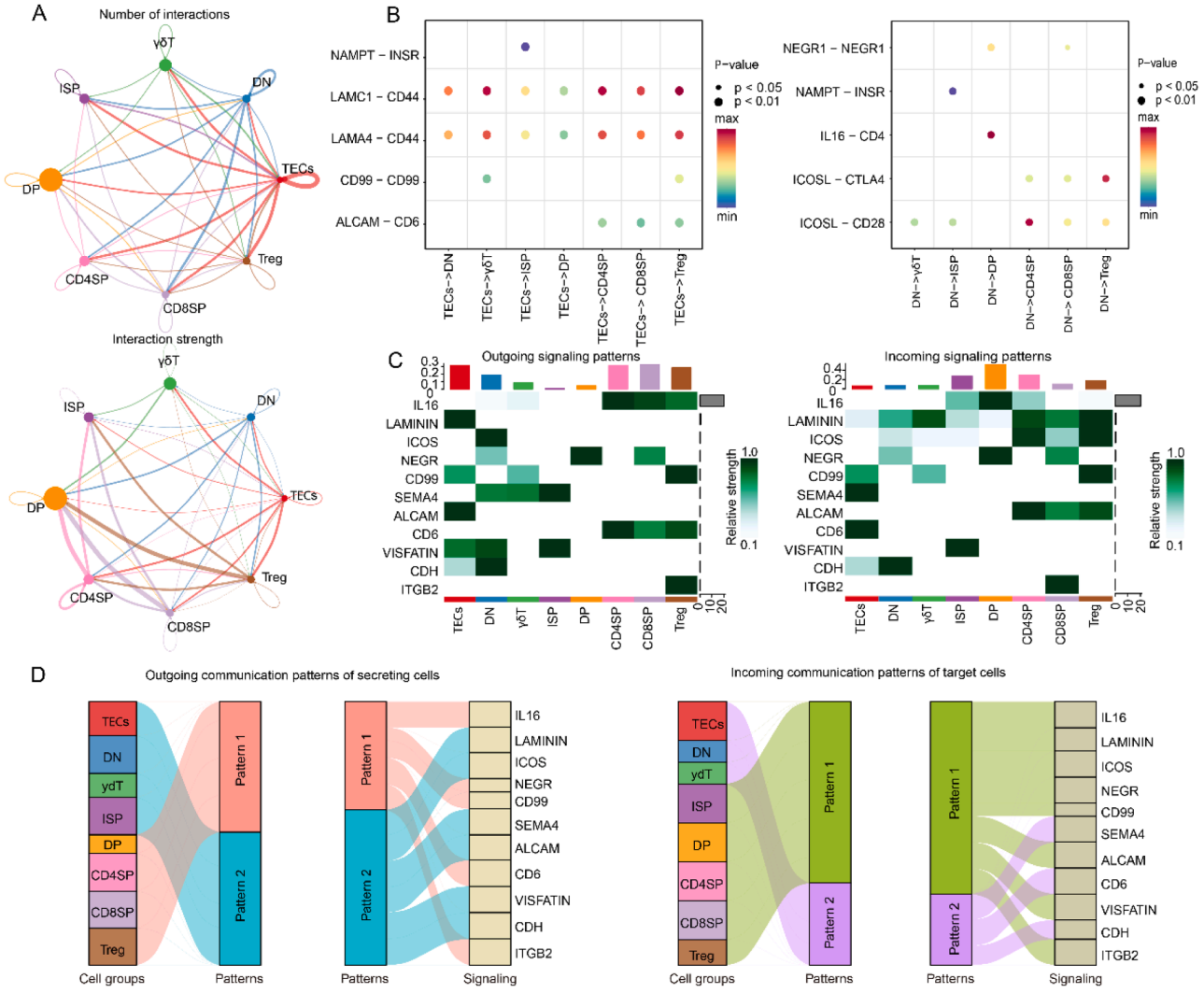

Fig. 6. Cell–cell communication networks between TEC and T cell populations. (A) Circle plots illustrating the interaction count and interaction strength between different cell populations. (B) Key ligand receptor interactions mediating communication between TEC and T cell subsets, and between DN cells and downstream T cell populations. (C) Outgoing and incoming signaling pathways across TEC and T cell subsets. (D) Pattern-based organization of outgoing and incoming cell–cell communication among TEC and T cell subsets.

collectively regulating T cell development and thymic selection.

Cross species comparative analysis of thymic cells from goose, human, and mouse

Integrative analysis of 11,882 strict one-to-one orthologous genes enabled systematic comparison of thymic cells from goose, human, and mouse (Table S3). UMAP embedding showed partial cell-type overlap but retained robust species-specific clustering, indicating persistent intrinsic transcriptional signatures despite orthology normalization (Fig. 7A).

Canonical marker annotation confirmed the presence of all major thymic cell types in each species (Figure S5). UMAP spatial arrangement revealed that macrophages, B cells, TECs, and early T cells (DN, ISP) were transcriptionally conserved, while later-stage T cells (DP, late DP, CD4SP, CD8SP, Treg) displayed pronounced species specificity-most notably among DP cells (Fig. 7B).

Compositional differences were observed in T cells subsets across species. DP cells predominated in goose and human, whereas DN and ISP cells were more enriched in mouse (Table S8, Fig. 7C). The proportion of γδ T cells was uniquely high in goose, highlighting avian-specific lineage bias. Developmental dynamics also differed: DP cell abundance decreased then increased with age in goose, whereas an opposite trend was observed in human and a postnatal increase and stabilization occurred in mouse (Fig. 7C).

Despite conserved developmental stages, significant interspecies transcriptional divergence was detected, especially at the DN and DP stages, which showed the highest numbers of differentially expressed genes. CD8SP subsets were more transcriptionally similar, while Treg cells showed pronounced mouse-specific signatures (Fig. 7D). Species-specific expression reflected distinct biological programs. Goose T cells were enriched for genes involved in cell adhesion/polarity (*ITGA1, PARD3B*), signaling regulation *(RASGEF1A, PRKD1, RPS6KA3*), and epigenetic modulation (*ESRR*G, *AFF2, DOT1L*). Human T cells upregulated stress adaptation and metabolic genes (*AQP3, HSPB1, DNAJB1, HSP90AB1*), especially at DN and Treg stages. Mouse T cells exhibited higher early developmental expression of cell cycle and metabolic genes (*NME4, CDK4, PHGDH, RAPGEF3, PDE4D*) (Fig. 7E).

In summary, while key milestones of T cell development are evolutionarily conserved, substantial species-specific differences in subset abundance, developmental dynamics, and molecular programs reveal evolutionary divergence in thymic cell fate and regulatory networks.

Discussion

Goose-specific and conserved features of thymic T cell development

This study integrates morphological characterization, single-cell transcriptomics, regulatory network inference, and cross-species comparative analyses to comprehensively define the developmental program of T cell differentiation in the goose thymus. Anatomically, the goose thymus exhibits a characteristic avian multi-lobulated, bead-like architecture that is established during embryogenesis, consistent with observations in other avian species (Ciriaco et al., 2003; Ma et al., 2013). Following hatching, the thymus undergoes rapid expansion accompanied by progressive corticomedullary compartmentalization, reaches peak size during mid-development, and subsequently undergoes age-associated involution. This dynamic progression reflects a conserved, non-linear trajectory of thymic development across vertebrates (Palmer, 2013).

Single-cell transcriptomic analysis showed that, despite marked morphological changes, the thymic cellular landscape remains predominantly T cell–centered throughout development, with only stage-specific variation in non–T cell populations (Klein et al., 2014). Thymic epithelial and myeloid cells maintain relatively stable proportions, supporting thymic architecture and the developmental microenvironment (Anderson and Takahama, 2012). Moreover, the presence of a complete DN, ISP, DP, SP continuum with canonical transcriptional features indicates a highly conserved trajectory of thymic T cell differentiation in the goose (Mingueneau et al., 2013).

Notably, γδ T cells are significantly enriched in the goose thymus compared with mammals. From a comparative immunological perspective, this expansion likely reflects a fundamental divergence in immune strategy between altricial mammals and precocial birds. Geese, as precocial species, hatch with a functionally mature immune system and face immediate environmental antigenic exposure. In contrast, mammals undergo a prolonged postnatal period of immune maturation. The expanded γδ T cell compartment in the goose thymus may serve to establish a robust peripheral surveillance network prior to the full maturation of the adaptive αβ T cell response. Mechanistically, this bias is reinforced by the increased *SOX13* regulon activity observed during the DN2b-to-DN3a transition, a regulatory node known to promote γδ lineage specification by stabilizing the TCRγδ locus and inhibiting αβ lineage commitment (Ciofani and Zúñiga-Pflücker, 2010; Hayday, 2009). Moreover, the abundance of γδ T cells in the avian thymus may also reflect a greater reliance on innate-like lymphocytes for early pathogen detection at mucosal barriers, a feature that may extend to other avian species and certain mammalian neonates with high environmental exposure (Dixon et al., 2021; Hu et al., 2023). Thus, the enrichment of γδ T cells in the goose thymus is not a stochastic species difference but likely represents an evolutionarily conserved adaptation aligned with life history traits and developmental timing.

DP cells remain the dominant T cell population across development, consistent with their central role in TCR selection and CD4/CD8 lineage differentiation (Starr et al., 2003). At the DP stage, thymic T cells bifurcate through a Late DP intermediate into CD4SP and CD8SP lineages, with CD4SP cells enriched for *CD4, GATA3, TCF7*, and migration-related genes, whereas CD8SP cells preferentially upregulate *CD8A, CD8*B, *RUNX3*, and effector-associated programs. Together, these findings highlight conserved differentiation logic alongside species-specific lineage dynamics in the goose thymus (Zhu et al., 2010) (Cruz-Guilloty et al., 2009). In summary, while the goose thymus follows the canonical framework of T cell differentiation, it also exhibits species-specific developmental dynamics and population composition features that reflect adaptive specialization.

Dynamic remodeling of regulatory networks during DN T cell development

Within a conserved framework, fine-resolution DN analysis revealed stepwise regulation of T cell lineage commitment and β-selection in the goose thymus. DN1–DN3 cells progress along a continuous trajectory from a progenitor-like state toward lineage commitment and β-selection readiness, with fate specification temporally uncoupled from TCR rearrangement. This progression is characterized by a sequential transcriptional program, including early enrichment of progenitor-associated factors (*BCL11A, TAL1, SPI1*), followed by activation of lineage-defining regulators (*BCL11B, NOTCH1, GATA3, TCF7*) and subsequent upregulation of β-selection–related genes (*RAG1/2, DNTT*, and TCR signaling components) (Rothenberg, 2019; Yui and Rothenberg, 2014). SCENIC analysis revealed dynamic remodeling of transcriptional regulatory networks during the DN stage, with distinct regulon activity patterns across DN subsets, indicating that T cell lineage commitment is driven by stage-specific transitions in regulatory architecture rather than a single transcription factor. Early DN stages show elevated activity of proliferative and progenitor-associated regulons (*CBFB* and *E2F7*) (Kent and Leone, 2019; Miller et al., 2001), followed by synchronous upregulation of lineage commitment–related regulons at the DN2b stage (*GATA3, TCF3, FOXP1*) (Engel and Murre, 2001; Feng et al., 2010; Hosoya et al., 2009). During DN3 progression, *LEF1*- and *TCF7*-associated regulon activity is further enhanced and linked to TCR rearrangement and signaling programs, supporting activation of the β-selection program (Rothenberg et al., 2008). Together, these results

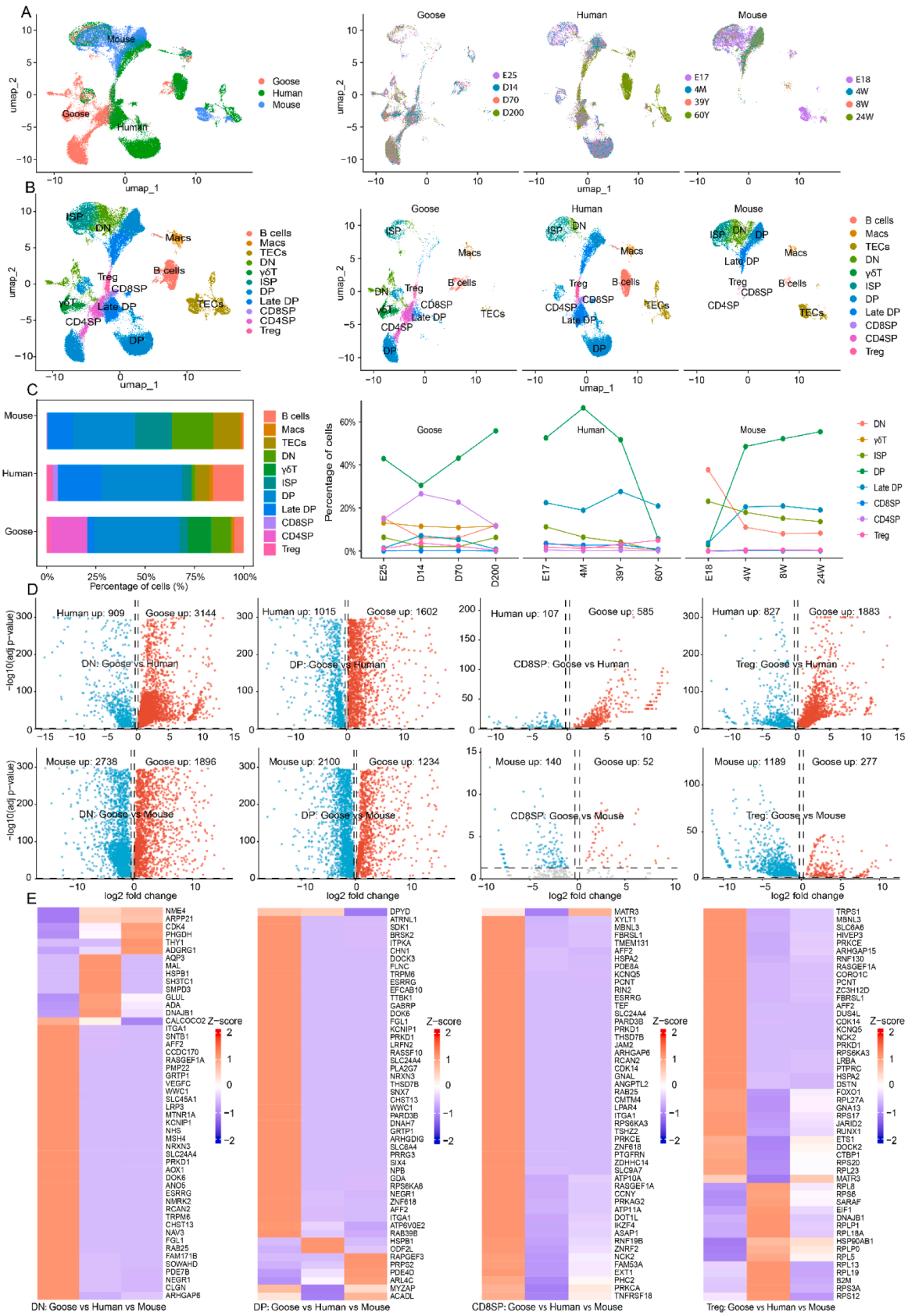

Fig. 7. Cross-species comparison of thymic cell composition, developmental dynamics, and transcriptional programs in goose, human, and mouse. (A) Integrated UMAP visualization of thymic cells across goose, human, and mouse. (B) Cross-species comparison of thymic cell-type composition and distribution. (C). Comparative dynamics of thymic T cell subsets across developmental stages in goose, human, and mouse. (D) Differential gene expression analysis of major T cell subsets between goose and human or mouse. (E) Conserved and species-specific transcriptional signatures of thymic T cell subsets.

define a stepwise regulatory framework for DN-stage T cell lineage commitment and β-selection in the goose thymus, highlighting dynamic transcriptional and regulon-level transitions.

Microenvironmental communication and species-specific divergence during thymic T cell development

Beyond cell-intrinsic regulation, cell–cell communication analysis highlights a cooperative role of the thymic microenvironment in T cell development. Thymic epithelial cells function as a central signaling hub, engaging multiple T cell subsets primarily through adhesion and extracellular matrix related pathways (e.g., LAMININ—CD44 and ALCAM-CD6), thereby supporting thymocyte positioning and maturation (Anderson and Takahama, 2012). In parallel, T cell communication shifts from signal production at early stages to signal integration at the DP stage, where DP cells show heightened connectivity, consistent with their role as a key checkpoint during thymic selection.

Cross-species comparison reveals a conserved framework of thymic T cell development among goose, human, and mouse, while highlighting clear divergence at the DP and subsequent stages, whereas early DN and ISP cells show greater cross-species overlap. Compared with mammals, goose T cells display sustained upregulation of gene modules related to cell adhesion, signal integration, and transcriptional regulation during mid-to-late development. This divergence may reflect species-specific constraints on thymic output kinetics. In precocial birds like the goose, the thymus must generate a functional and diverse T cell repertoire within a compressed developmental window prior to hatching. The extended activation of adhesion and signaling modules in DP cells may therefore represent a mechanism to enhance the efficiency of positive and negative selection, ensuring timely production of competent naïve T cells. Together, these findings delineate the developmental landscape of goose thymic T cells and identify the DP and later stages as key windows for species-specific regulatory programs, underscoring the adaptive plasticity of immune development in response to life history strategy.

Conclusion

This study integrates histological analysis, single-cell transcriptomics, and regulatory network inference to construct a high-resolution atlas of thymic development in the ZW goose. While the overall framework of T cell development is conserved across vertebrates, the goose thymus displays distinct species-specific features in cellular composition, developmental dynamics, and regulatory programs, including a bias toward the γδ T cell lineage. Thymic epithelial cells shape the thymic niche through adhesion- and microenvironment-related signaling, whereas DP and mature T cells emerge as key hubs for signal integration. Together, these findings provide a comprehensive cellular and molecular framework for avian thymic T cell development and offer a valuable resource for comparative immunology and immunological studies in waterfowl.

Funding

This work was supported by the National Key Research and Development Program of China (2023YFD1300304), the National Natural Science Foundation of China (32302729), the China Agriculture Research System of MOF and MARA (CARS-42-7), the SAAS Program for Excellent Research Team (2022-021), and the Key Research and Development Program of Ningbo (2023Z126).

AI tool disclosure

During the preparation of this work, the authors used ChatGPT (OpenAI, GPT-3.5) solely for the purpose of improving language accuracy and readability. After using this tool, the authors reviewed and edited the content as needed and take full responsibility for the publication's content.

Scientific section

Genetics and molecular biology.

CRediT authorship contribution statement

Cui Wang: Writing – review & editing, Writing – original draft, Validation, Resources, Project administration, Methodology, Investigation, Funding acquisition, Formal analysis, Conceptualization. **Zuoyin Zhu:** Writing – review & editing, Writing – original draft, Validation, Software, Methodology, Formal analysis, Data curation, Conceptualization. **Yi Liu:** Resources, Investigation, Data curation. **Yongping Yang:** Writing – review & editing, Resources, Conceptualization. **Shufang Chen:** Resources, Funding acquisition, Data curation. **Daqian He:** Writing – review & editing, Funding acquisition.

Disclosures

The authors declare that they have no known competing financial interests or personal relationships that could have appeared to influence the work reported in this paper.

Supplementary materials

Supplementary material associated with this article can be found, in the online version, at doi:10.1016/j.psj.2026.106951.

Data availability

The raw and processed scRNA-seq data generated in this study are available in the GEO database under accession number GSE315444. Public datasets used in this study include human thymus scRNA-seq data from GSA-Human (HRA007980) and mouse thymus scRNA-seq data from ArrayExpress (E-MTAB-8581). All other data are available within the article, supplementary information, or source data files.

References

Aibar, S., González-Blas, C.B., Moerman, T., Huynh-Thu, V.A., Imrichova, H., Hulselmans, G., Rambow, F., Marine, J.-C., Geurts, P., Aerts, J., van den Oord, J., Atak, Z.K., Wouters, J., Aerts, S., 2017. SCENIC: single-cell regulatory network inference and clustering. Nat. Methods 14 (11), 1083–1086. https://doi.org/10.1038/nmeth.4463.

Anderson, G., Takahama, Y., 2012. Thymic epithelial cells: working class heroes for T cell development and repertoire selection. Trends Immunol. 33 (6), 256–263. https://doi.org/10.1016/j.it.2012.03.005.

Boehme, L., Roels, J., Taghon, T., 2022. Development of γδ T cells in the thymus – a human perspective. Semin. Immunol. 61-64, 101662. https://doi.org/10.1016/j.smim.2022.101662.

Campbell, L.K., Magor, K.E., 2020. Pattern recognition receptor signaling and innate responses to influenza A viruses in the Mallard Duck, compared to humans and chickens. Front. Cell Infect. Microbiol. 10, 209. https://doi.org/10.3389/fcimb.2020.00209.

Cao, J., Spielmann, M., Qiu, X., Huang, X., Ibrahim, D.M., Hill, A.J., Zhang, F., Mundlos, S., Christiansen, L., Steemers, F.J., Trapnell, C., Shendure, J., 2019. The single-cell transcriptional landscape of mammalian organogenesis. Nature 566 (7745), 496–502. https://doi.org/10.1038/s41586-019-0969-x.

Chen, C.L., Bucy, R.P., Cooper, M.D., 1990. T cell differentiation in birds. Semin. Immunol. 2 (1), 79–86.

Ciofani, M., Zúñiga-Pflücker, J.C., 2007. The thymus as an inductive site for T lymphopoiesis. Annu Rev. Cell Dev. Biol. 23, 463–493. https://doi.org/10.1146/annurev.cellbio.23.090506.123547.

Ciofani, M., Zúñiga-Pflücker, J.C., 2010. Determining γδ versus αβ T cell development. Nat. Rev. Immunol. 10 (9), 657–663. https://doi.org/10.1038/nri2820.

Ciriaco, E., Píñera, P.P., Díaz-Esnal, B., Laurà, R., 2003. Age-related changes in the avian primary lymphoid organs (thymus and bursa of Fabricius). Microsc. Res. Tech. 62 (6), 482–487. https://doi.org/10.1002/jemt.10416.

Cruz-Guilloty, F., Pipkin, M.E., Djuretic, I.M., Levanon, D., Lotem, J., Lichtenheld, M.G., Groner, Y., Rao, A., 2009. Runx3 and T-box proteins cooperate to establish the transcriptional program of effector CTLs. J. Exp. Med. 206 (1), 51–59. https://doi.org/10.1084/jem.20081242.

Dixon, R., Preston, S.G., Dascalu, S., Flammer, P.G., Fiddaman, S.R., McLoughlin, K., Boyd, A., Volf, J., Rychlik, I., Bonsall, M.B., Kaspers, B., Smith, A.L., 2021. Repertoire analysis of γδ T cells in the chicken enables functional annotation of the genomic region revealing highly variable pan-tissue TCR gamma V gene usage as well as identifying public and private repertoires. BMC Genom. 22 (1), 719. https://doi.org/10.1186/s12864-021-08036-9.

Dumlu, B., 2024. The global goose meat production quantity forecast for the 2023–2027 years. Selcuk J. Agric. Food Sci. 38 (2), 326–341. https://doi.org/10.15316/SJAFS.2024.030.

Durinck, S., Spellman, P.T., Birney, E., Huber, W., 2009. Mapping identifiers for the integration of genomic datasets with the R/bioconductor package biomaRt. Nat. Protoc. 4 (8), 1184–1191. https://doi.org/10.1038/nprot.2009.97.

Eickhoff, S., Brewitz, A., Gerner, M.Y., Klauschen, F., Komander, K., Hemmi, H., Garbi, N., Kaisho, T., Germain, R.N., Kastenmüller, W., 2015. Robust anti-viral immunity requires multiple distinct T cell-dendritic cell interactions. Cell 162 (6), 1322–1337. https://doi.org/10.1016/j.cell.2015.08.004.

Engel, I., Murre, C., 2001. The function of E- and id proteins in lymphocyte development. Nat. Rev. Immunol. 1 (3), 193–199. https://doi.org/10.1038/35105060.

Feng, X., Ippolito, G.C., Tian, L., Wiehagen, K., Oh, S., Sambandam, A., Willen, J., Bunte, R.M., Maika, S.D., Harriss, J.V., Caton, A.J., Bhandoola, A., Tucker, P.W., Hu, H., 2010. Foxp1 is an essential transcriptional regulator for the generation of quiescent naive T cells during thymocyte development. Blood 115 (3), 510–518. https://doi.org/10.1182/blood-2009-07-232694.

Flajnik, M.F., Kasahara, M., 2010. Origin and evolution of the adaptive immune system: genetic events and selective pressures. Nat. Rev. Genet. 11 (1), 47–59. https://doi.org/10.1038/nrg2703.

Germain, P.L., Lun, A., Garcia Meixide, C., Macnair, W., Robinson, M.D., 2021. Doublet identification in single-cell sequencing data using scDblFinder. F1000Res 10, 979. https://doi.org/10.12688/f1000research.73600.2.

Hayday, A.C., 2009. γδ T cells and the lymphoid stress-surveillance response. Immunity 31 (2), 184–196. https://doi.org/10.1016/j.immuni.2009.08.006.

Hosoya, T., Kuroha, T., Moriguchi, T., Cummings, D., Maillard, I., Lim, K.C., Engel, J.D., 2009. GATA-3 is required for early T lineage progenitor development. J. Exp. Med. 206 (13), 2987–3000. https://doi.org/10.1084/jem.20090934.

Hu, Y., Hu, Q., Li, Y., Lu, L., Xiang, Z., Yin, Z., Kabelitz, D., Wu, Y., 2023. γδ T cells: origin and fate, subsets, diseases and immunotherapy. Signal Transduct. Target. Ther. 8 (1), 434. https://doi.org/10.1038/s41392-023-01653-8.

Jin, S., Guerrero-Juarez, C.F., Zhang, L., Chang, I., Ramos, R., Kuan, C.-H., Myung, P., Plikus, M.V., Nie, Q., 2021. Inference and analysis of cell-cell communication using CellChat. Nat. Commun. 12 (1), 1088. https://doi.org/10.1038/s41467-021-21246-9.

Kent, L.N., Leone, G., 2019. The broken cycle: E2F dysfunction in cancer. Nat. Rev. Cancer 19 (6), 326–338. https://doi.org/10.1038/s41568-019-0143-7.

Kernfeld, E.M., Genga, R.M.J., Neherin, K., Magaletta, M.E., Xu, P., Maehr, R., 2018. A single-cell transcriptomic atlas of Thymus organogenesis resolves cell types and developmental maturation. Immunity 48 (6). https://doi.org/10.1016/j.immuni.2018.04.015, 1258-1270.e1256.

Klein, L., Kyewski, B., Allen, P.M., Hogquist, K.A., 2014. Positive and negative selection of the T cell repertoire: what thymocytes see (and don't see). Nat. Rev. Immunol. 14 (6), 377–391. https://doi.org/10.1038/nri3667.

Korsunsky, I., Millard, N., Fan, J., Slowikowski, K., Zhang, F., Wei, K., Baglaenko, Y., Brenner, M., Loh, P.R., Raychaudhuri, S., 2019. Fast, sensitive and accurate integration of single-cell data with Harmony. Nat. Methods 16 (12), 1289–1296. https://doi.org/10.1038/s41592-019-0619-0.

Lai, F.-Y., Chang, K.-C., Chang, C.-S., Wang, P.-H., 2022. Development of a rapid sex identification method for newborn pigeons using recombinase polymerase amplification and a lateral-flow dipstick on farm. Animals 12 (21), 2969.

Li, B., Li, W., Tian, Y., Guo, S., Qian, L., Xu, D., Cao, N., 2020. Selenium-alleviated hepatocyte necrosis and DNA damage in cyclophosphamide-treated geese by mitigating oxidative stress. Biol. Trace Elem. Res. 193 (2), 508–516. https://doi.org/10.1007/s12011-019-01717-3.

Li, Y., Li, H., Peng, C., Meng, G., Lu, Y., Liu, H., Cui, L., Zhou, H., Xu, Z., Sun, L., Liu, L., Xiong, Q., Sun, B., Jiao, S., 2024. Unraveling the spatial organization and development of human thymocytes through integration of spatial transcriptomics and single-cell multi-omics profiling. Nat. Commun. 15 (1), 7784. https://doi.org/10.1038/s41467-024-51767-y.

Li, Y., Zeng, W., Li, T., Guo, Y., Zheng, G., He, X., Bai, L., Ding, G., Jin, L., Liu, X., 2021. Integrative single-cell transcriptomic analysis of human fetal thymocyte development. Front. Genet. 12, 679616. https://doi.org/10.3389/fgene.2021.679616.

Liu, G., Zhou, L., Zhang, L., Luo, Z., Xu, W., 2013. The complete mitochondrial genome of bean goose (Anser fabalis) and implications for anseriformes taxonomy. PLoS One 8 (5), e63334. https://doi.org/10.1371/journal.pone.0063334.

Ma, D., Wei, Y., Liu, F., 2013. Regulatory mechanisms of thymus and T cell development. Dev. Comp. Immunol. 39 (1), 91–102. https://doi.org/10.1016/j.dci.2011.12.013.

Medeiros, N.C., Santos Filho, E.N.D., Ayres, D.A.S., Cancio, B., Smaniotto, S., Reis, M., Lins, M.P., 2025. Involvement of CXCL12/CXCR4 pair in migration of thymocytes from lactating mice. J. Reprod. Immunol. 168, 104444. https://doi.org/10.1016/j.jri.2025.104444.

Melichar, H.J., Narayan, K., Der, S.D., Hiraoka, Y., Gardiol, N., Jeannet, G., Held, W., Chambers, C.A., Kang, J., 2007. Regulation of γδ versus αβ T lymphocyte differentiation by the transcription factor SOX13. Science 315 (5809), 230–233. https://doi.org/10.1126/science.1135344.

Miller, J.D., Stacy, T., Liu, P.P., Speck, N.A., 2001. Core-binding factor β (CBFβ), but not cbfβ–smooth muscle myosin heavy chain, rescues definitive hematopoiesis in cbfβ-deficient embryonic stem cells. Blood 97 (8), 2248–2256. https://doi.org/10.1182/blood.V97.8.2248.

Mingueneau, M., Kreslavsky, T., Gray, D., Heng, T., Cruse, R., Ericson, J., Bendall, S., Spitzer, M.H., Nolan, G.P., Kobayashi, K., von Boehmer, H., Mathis, D., Benoist, C., Best, A.J., Knell, J., Goldrath, A., Jojic, V., Koller, D., Shay, T., 2013. The transcriptional landscape of αβ T cell differentiation. Nat. Immunol. 14 (6), 619–632. https://doi.org/10.1038/ni.2590.

Palmer, D.B., 2013. The effect of age on thymic function. Front. Immunol. 4, 316. https://doi.org/10.3389/fimmu.2013.00316.

Park, J.E., Botting, R.A., Domínguez Conde, C., Popescu, D.M., Lavaert, M., Kunz, D.J., Goh, I., Stephenson, E., Ragazzini, R., Tuck, E., Wilbrey-Clark, A., Roberts, K., Kedlian, V.R., Ferdinand, J.R., He, X., Webb, S., Maunder, D., Vandamme, N., Mahbubani, K.T., Polanski, K., Teichmann, S.A., 2020. A cell atlas of human thymic development defines T cell repertoire formation. Science 367 (6480), eaay3224. https://doi.org/10.1126/science.aay3224.

Qiu, X., Mao, Q., Tang, Y., Wang, L., Chawla, R., Pliner, H.A., Trapnell, C., 2017. Reversed graph embedding resolves complex single-cell trajectories. Nat. Methods 14 (10), 979–982. https://doi.org/10.1038/nmeth.4402.

Ratcliffe, M.J., 2006. Antibodies, immunoglobulin genes and the bursa of Fabricius in chicken B cell development. Dev. Comp. Immunol. 30 (1–2), 101–118. https://doi.org/10.1016/j.dci.2005.06.018.

Ren, T., Liang, S., Zhao, A., He, K., 2016. Analysis of the complete mitochondrial genome of the Zhedong White goose and characterization of NUMTs: reveal domestication history of goose in China and Euro. Gene 577 (1), 75–81. https://doi.org/10.1016/j.gene.2015.11.018.

Ribatti, D., Tamma, R., Elieh Ali Komi, D., 2019. The morphological basis of the development of the chick embryo immune system. Exp. Cell Res. 381 (2), 323–329. https://doi.org/10.1016/j.yexcr.2019.05.027.

Rodrigues, P.M., Sousa, L.G., Alves, N.L., 2025. Cortical thymic epithelial cells: key developers of the code of T-cell selection and TCR repertoire diversity. Immunol. Rev. 332 (1), e70049. https://doi.org/10.1111/imr.70049.

Rothenberg, E.V., 2019. Programming for T-lymphocyte fates: modularity and mechanisms. Genes Dev. 33 (17–18), 1117–1135. https://doi.org/10.1101/gad.327163.119.

Rothenberg, E.V., Moore, J.E., Yui, M.A., 2008. Launching the T-cell-lineage developmental programme. Nat. Rev. Immunol. 8 (1), 9–21. https://doi.org/10.1038/nri2232.

Shim, C.H., Cho, S., Shin, Y.M., Choi, J.M., 2022. Emerging role of bystander T cell activation in autoimmune diseases. BMB Rep. 55 (2), 57–64. https://doi.org/10.5483/BMBRep.2022.55.2.183.

Starr, T.K., Jameson, S.C., Hogquist, K.A., 2003. Positive and negative selection of T cells. Annu. Rev. Immunol. 21, 139–176. https://doi.org/10.1146/annurev.immunol.21.120601.141107.

Stuart, T., Butler, A., Hoffman, P., Hafemeister, C., Papalexi, E., Mauck 3rd, W.M., Hao, Y., Stoeckius, M., Smibert, P., Satija, R., 2019. Comprehensive integration of single-cell data. Cell 177 (7), 1888–1902. https://doi.org/10.1016/j.cell.2019.05.031 e1821.

Takaba, H., Takayanagi, H., 2017. The mechanisms of T cell selection in the Thymus. Trends. Immunol. 38 (11), 805–816. https://doi.org/10.1016/j.it.2017.07.010.

Takahama, Y., 2006. Journey through the thymus: stromal guides for T-cell development and selection. Nat. Rev. Immunol. 6 (2), 127–135. https://doi.org/10.1038/nri1781.

Trapnell, C., Cacchiarelli, D., Grimsby, J., Pokharel, P., Li, S., Morse, M., Lennon, N.J., Livak, K.J., Mikkelsen, T.S., Rinn, J.L., 2014. The dynamics and regulators of cell fate decisions are revealed by pseudotemporal ordering of single cells. Nat. Biotechnol. 32 (4), 381–386. https://doi.org/10.1038/nbt.2859.

Webster, R.G., Bean, W.J., Gorman, O.T., Chambers, T.M., Kawaoka, Y., 1992. Evolution and ecology of influenza A viruses. Microbiol. Rev. 56 (1), 152–179. https://doi.org/10.1128/mr.56.1.152-179.1992.

Yui, M.A., Rothenberg, E.V., 2014. Developmental gene networks: a triathlon on the course to T cell identity. Nat. Rev. Immunol. 14 (8), 529–545. https://doi.org/10.1038/nri3702.

Zheng, G.X.Y., Terry, J.M., Belgrader, P., Ryvkin, P., Bent, Z.W., Wilson, R., Ziraldo, S.B., Wheeler, T.D., McDermott, G.P., Zhu, J., Gregory, M.T., Shuga, J., Montesclaros, L., Underwood, J.G., Masquelier, D.A., Nishimura, S.Y., Schnall-Levin, M., Wyatt, P.W., Hindson, C.M., Bielas, J.H., 2017. Massively parallel digital transcriptional profiling of single cells. Nat. Commun. 8 (1), 14049. https://doi.org/10.1038/ncomms14049.

Zhu, J., Yamane, H., Paul, W.E., 2010. Differentiation of effector CD4 T cell populations (*). Annu. Rev. Immunol. 28, 445–489. https://doi.org/10.1146/annurev-immunol-030409-101212.